Methods for precise photoelectron counting with photomultipliers

R. Dossi[a], A. Ianni[a,c], G. Ranucci[d], O. Ju. Smirnov[b,d].

a) Laboratori Nazionali del Gran Sasso - Assergi (Aq) - Italy

b) Joint. Inst. for Nuclear Research - Dubna - Russia

c) University of L'Aquila, Physics Department - Coppito di L'Aquila - Italy

d) I.N.F.N. Sezione di Milano - Via Celoria (MI) - Italy

Abstract

A series of measurements has been performed on a THORN EMI 9351 photomultipliers in order to investigate its response to a low light intensity. The precision of the different procedures to determine the photoelectrons number have been studied. The data show that the various approaches give consistent and reliable results, thus allowing the precise calibration of the device for applications of photon counting.

PACS number(s): 29.40.Mc; 85.60.Ma

Keywords: photomultiplier, photoelectron, scintillator, calibration

Corresponding author:

Oleg Yu. Smirnov

e-mail: smirnov@lngs.infn.it,smipol@cv.jinr.ru

1 Introduction

In many experimental conditions involving scintillators and photomultipliers the light pulse arriving at the photocathode contains very few photons. The mean value μ of the Poisson distributed number of photoelectrons detected per burst depends on various factors, the most important being the energy of the incident particle in the scintillator, the geometrical coverage of the photocathode, and the quantum and collection efficiency of the phototube. In a given experimental occurrence the precise evaluation of μ can be accomplished with different methods, based on the use of the informations contained in the output of the phototube.

In the present paper we present the results of an investigation carried out to evaluate and compare different methods of mean p.e. number estimation from the PMT charge distribution. We studied the charge spectrum of the Thorn EMI 9351 PMT expected to be used in the Borexino experiment. In Borexino an organic liquid scintillator is used to detect the ^7Be solar neutrinos through the electron-neutrino elastic scattering. A rate of few p.e. per PMT is expected.

In order to study the response of the PMT for various levels of a light intensity we used neutral optical filters (not changing the spectral characteristic of the radiation) to control the amount of the incident light in different measurements.

In table 1 the declared properties of the filters used are summarized where $\tau = \frac{\Phi_T}{\Phi_0}$ is the ratio of the transmitted to the incident luminous flux and D=$\log \frac{1}{\tau}$ is the so called optical density.

The discussion of the obtained results follows the next plan. In Sec. 2 we underline the features of the PMT charge signal, that are important for the development of a PMT charge response model. In Sec. 3 we discuss the method of Single Electron Response (SER) parameters evaluation from the PMT response to a low intensity light source. In Sec. 4 we present different methods of mean number of p.e. evaluation from the PMT charge spectra and in Sec. 5 we analyze the measurements. Sec. 6 contains the conclusions.

2 The PMT charge response to a low intensity light source

The charge response of the PMTs for a low intensity light has been studied using the Borexino PMTs test facility at the Gran Sasso Laboratories. The experimental set-up is shown in fig. 1. A Hamamatsu pulse laser (0.39 mW peak power, 27.3 ps pulse width, 415 nm wavelength, which is close to the maximum quantum efficiency of Thorn EMI 9351) has been used to study the PMT charge spectrum. Using the laser internal trigger the ADC gate was generated as it is shown in the same figure. The light pulse from the laser is delivered by a 6 meters long optic fiber into the dark-room. Between the fiber and the PMT an optical filters support is placed. The dark noise spectrum has also been studied with the laser turned off using for the ADC gate the PMT signal discriminated at the level of 0.05-0.10 p.e. in order to cut the electronics noise.

We have performed a set of measurements with different filters using the same PMT, which was placed inside a μ-metal shield in order to screen the Earth's Magnetic field.

The first step of the procedure to determine the mean number of detected photoelectrons requires the precise determination of the single response (SER) of the phototube.

Assuming a Poisson distribution for the p.e. number leaving the photocathode [2], one can write:

$$\frac{P(2)}{P(1)} = \frac{\mu}{2}, \tag{2}$$

where P(2) and P(1) are the probability to detect two or one p.e. respectively and μ is the mean value of p.e. Therefore, in order to keep the PMT charge multiphotoelectrons responses at the 1% level it is necessary to have $\mu \leq 0.02$. Taking the PMT charge spectrum, we controlled this number using the probability to have zero p.e.:

$$P(0) = \frac{N_{ped}}{N_{trig}} = e^{-\mu}, \tag{3}$$

where N_{ped} is the number of events in the pedestal (i.e. the response when no p.e. leaves the photocathode) and N_{trig} is the number of laser triggers.

For small μ the output of the PMT could be altered by the dark noise of the PMT, which is of the order of some KHz. Because of the dark noise a number of random coincidences can be detected, expressed by:

$$f_{random} = f_{dark} \cdot f_{trig} \cdot \tau_{gate}, \tag{4}$$

where f_{random} is the random coincidence rate, f_{dark} is the dark noise rate and τ_{gate} is the ADC gate. On the other hand for small μ the event rate is, using (3):

$$f_{events} = (1 - P(0)) \cdot f_{trig} \simeq \mu \cdot f_{trig} \tag{5}$$

Therefore, in order to have the random coincidences' contribution at the level of 1% it is necessary to keep:

$$\mu \geq \frac{f_{dark} \cdot \tau_{gate}}{0.01} \tag{6}$$

For 2 KHz dark rate and $\tau_{gate} = 80$ns (6) gives $\mu \geq 0.016$. So for $\mu = 0.02$ a PMT response has both a negligible contribution of the dark noise spectrum and of the multiphotoelectrons one.

In fig. 2 a typical PMT charge spectrum together with the dark noise one for the same PMT is shown. The threshold during the data taking was set at the level of 0.15 p.e. Comparing these spectra one can point out that a longer tail and a higher contribution of small amplitude pulses distinguish the dark noise spectrum. The origin of the longer tail events is the Čerenkov light of cosmic particles and scintillation caused by natural radioactivity contamination in the PMT glass bulb [3].

The contribution of the small amplitude pulses in literature is usually assigned to the thermoionic noise from dynodes. In order to check this assumption we grounded the first dynode and kept the photocathode at a small positive potential. In this way the possible noise from the dynodes system

was measured. The obtained spectrum (presented in fig. 2) does not fit the difference between the spectra. The most probable origin of this difference is the thermoionic emission from the photocathode material (SbCsK) remaining the inner parts of the PMT during the technological procedure of the photocathode deposition. Photoelectrons emitted from the inner parts arrive to the first dynode with a smaller energy or under unfavorable angles of incidence, giving a rise to the probability of elastic scattering and backscattering from the first dynode ([4],[5]).

We would like to underline the following:

- a significant amount of small amplitude pulses in the charge spectra is an intrinsic property of the EMI 9135 PMT, and it should be taken into account when modeling the SER;
- a significant difference between the SER and the dark-noise makes impossible to use the latter distribution for the precise PMT calibration;
- the response of the PMT for a low intensity light source is not a pure SER as, due to the statistical nature of the light counting, there is always a certain amount of multiple p.e. counting with a total probability $1 - P(0) - P(1)$, where $P(0)$ is the probability of no response and $P(1)$ is the probability of a SER.

3 The SER charge spectrum parameters

As it has been mentioned, even for small μ, the PMT charge spectrum is not a pure SER. In order to extract the SER spectrum, i.e. the ideal PMT response to a single p.e. hitting the first dynode, the pedestal and multiple p.e. response should be rejected from the experimental charge spectrum. An ideal SER model has been successfully applied for such separation of the different parts of real PMT spectrum.

The main parameters of interest for the ideal SER are the mean value x_1 of the ideal SER itself and its relative variance $v_1 = (\sigma_1/x_1)^2$, where σ_1 is the ideal SER standard deviation.

3.1 The SER model and fitting function for the PMT response for small μ

An ideal SER model consisting of a gaussian and an exponential has been used:

$$SER_0(x) = \begin{cases} \frac{p_E}{A} e^{-\frac{x-x_p}{A}} + \frac{1}{\sqrt{2\pi}\sigma_0} \frac{1-p_E}{g_N} e^{-\frac{1}{2}(\frac{x-x_0-x_p}{\sigma_0})^2} & x > x_p \\ 0 & x \leq x_p \end{cases} \quad (7)$$

with the following parameters:

- A is the slope of the exponential part of the $SER_0(x)$
- p_E is the fraction of events under the exponential function,
- x_p is the pedestal position,

- x_0 and σ_0 the mean value and the standard deviation of the gaussian part of the single p.e. response respectively;

and the factor

$$g_N = \frac{1}{2}\Big(1 + Erf\Big(\frac{x_0}{\sqrt{2}\sigma}\Big)\Big)$$

which takes account for the cut of the PMT response gaussian part. $Erf(x)$ is the error function.

The model has been checked on the number of different PMTs; the good quality of the final fit justify our choice of the $SER_0(x)$ function.

To account for the electronics noise one should perform the convolution of the ideal SER with a noise function, $Noise(x)$:

$$SER(x) = SER_0(x) \otimes Noise(x), \tag{8}$$

where:

$$Noise(x) = \frac{1}{\sqrt{2\pi}\sigma_p} e^{-\frac{1}{2}(\frac{x-x_p}{\sigma_p})^2}, \tag{9}$$

which fits the pedestal with a proper normalization. The convolution does not influence the gaussian part of the SER since $\sigma_1 >> \sigma_p$ (in our measurements $\sigma_p \sim 0.01\sigma_1$), but it does the exponential one which is closer to the pedestal. The analytical formula for the convolution of the exponential function with the gaussian is:

$$\frac{p_E}{2A} \cdot e^{\frac{\sigma_p^2 - 2A(x-x_p)}{2A^2}} \cdot \Big(1 + Erf\Big(\frac{A(x-x_p) - \sigma_p^2}{\sqrt{2}A\sigma_p}\Big)\Big), \tag{10}$$

The PMT response for a low light intensity contains a certain amount of signals coming from the multiple primary p.e. Assuming the linearity of the PMT response one can write: $x_n = nx_1$ and $\sigma_n = \sqrt{n}\sigma_1$, where x_n and σ_n are the mean value and the standard deviation of the PMT response to n-p.e., respectively. Taking into account the Poisson distribution of the detected light and using a gaussian approximation for the responses to $Np.e. > 2$ (the validity of this assumption is discussed later), the multi-p.e. response will have the following form:

$$M(x) = \sum_{n=2}^{N_M} \frac{P(n;\mu)}{\sqrt{2n\pi}\sigma_1} e^{-\frac{1}{2n}\left(\frac{x-nx_1-x_p}{\sigma_1}\right)^2} \tag{11}$$

where the response to n p.e. is approximated by a gaussian and $P(n;\mu)$ is the Poisson distribution with mean value μ to account for the different contributions of $0 \to n$ p.e. In (11) N_M, the maximum number of multiple-p.e. responses considered, depends on μ and on the ADC scale. The function $M(x)$ has three additional parameters μ, x_1 and σ_1.

For fitting the PMT response to a low intensity light source (small μ) with a small contribution of multiple-p.e. approximate values of x_1 and σ_1 can be used:

$$x_1 \approx (1 - p_E) \cdot x_0 + p_E A \tag{12}$$

$$\sigma_1 \approx (1 - p_E) \cdot (\sigma_0^2 + x_0^2) + 2p_E A^2 - x_1^2. \tag{13}$$

The approximate character of these formulae come from the cut in the gaussian part of the SER, whose portion below 0 is truncated.

A more complex analytical approach has been developed for bigger μ with lower statistics data, which gives a precise value of x_1 and σ_1 (see appendix A). Here we are following the standard procedure of the SER definition described in literature [9], making corrections for the multiple p.e. signals and contribution of the small amplitude pulses in single p.e. response.

From (8), (9) and (11) the fitting function for the PMT spectrum can be written as:

$$f(x) = N_0 \cdot (P(0) \cdot Noise(x) + P(1) \cdot SER(x) + M(x)) \tag{14}$$

where N_0 is a normalization factor.

Using (14) for fitting the SER data, only the $SER(x)$ parameters (x_0, σ_0, p_E and A) are free. When used with small μ, this function will work well only for very high statistics because of the big $P(0)$ probability.

We should point out that (14) was introduced only to separate the contribution of small amplitude pulses from the events in pedestal. Its use is limited to the case of small μ (~ 0.02) and high statistics data. For 1% precision of μ definition at 1σ c.l. the necessary statistics is $5 \cdot 10^5$ (see appendix B). The statistics needed for a 1% precision of the SER parameters definition is of the order of 10^5 excluding the events in pedestal (see appendix A). So for $\mu \sim 0.02$ the total number of events should be $5 \cdot 10^6$.

3.2 The SER charge spectrum parameters

In order to obtain the SER parameters x_1 and v_1 the following procedure has been applied.

1. **approximate evaluation of μ**

   Using (3) an approximate value of μ has been defined evaluating the ratio of the events under the gaussian fitting the pedestal to the total number of triggers.

2. **fitting of experimental spectrum**

   The fit of the experimental data with (14) has been performed with fixed μ (see fig. 3).

3. **evaluation of the parameters of charge spectrum**

   The mean value, x_m^*, and the r.m.s., σ_m^*, have been defined for the experimental spectrum after the pedestal rejection. To reject the pedestal events the experimental data have been used for $x > x_p + 5 \cdot \sigma_p$, while the data have been replaced by the fitting curve (see black-painted area in fig. 4) for $x < x_p + 5 \cdot \sigma_p$.

4. **precise evaluation of μ**

   The number of pedestal events have been estimated from the difference between the total number of triggers and the events under the modeling curve (see fig. 4), then the precise μ value has been obtained using (3).

5. **calibration: evaluation of SER parameters**

   x_1 and v_1 (the SER relative variance) have been obtained from x_m^* and $v_m^* = (\sigma_m^*/x_m^*)^2$ (the PMT charge spectrum relative variance) discarding the contribution of the multiple-hits, using the formulae (see appendix C):

$$x_1 = x_m^*(1 - \frac{\mu}{2}) \tag{15}$$

$$v_1 = \frac{v_m^* - \frac{\mu}{2}}{1 - \frac{\mu}{2}} \tag{16}$$

4 Mean p.e. number estimation

Four procedures of the mean p.e. number estimation from the PMT charge spectrum have been studied:

1. **using the Poisson probability of no responce**

   Assuming the Poisson distribution of the detected light, the mean p.e. number can be defined from (3):

$$\mu = -ln(P(0)).$$

2. **using the calibration value**

   Assuming in addition the linearity of the PMT, the electronics used and the ADC, the mean number of p.e. can be estimated from the mean value of the charge spectra using the calibration of the SER:

$$\mu = \frac{x_m}{x_1}, \tag{17}$$

   where mean value

$$x_m = \frac{\sum N(i) \cdot i}{\sum N(i)}, \tag{18}$$

   is defined over all spectrum, including pedestal. N(i) is the content of the i-th bin of the charge histogram.

3. **using the relative variance of the charge spectra and SER parameters**

   The mean p.e. number can be estimated from the relative variance of the charge spectra. For assumption involved see [2]. If v_1 is the relative variance of the SER spectrum, then:

$$v = (\frac{\sigma_m}{x_m})^2 = \frac{1 + v_1}{\mu},$$

   i.e.

$$\mu = \frac{1 + v_1}{v}. \tag{19}$$

4. **applying fit of the charge spectra based on the SER function**

   Keeping all the above mentioned assumptions and assuming the mutual independence of the contributions of the primary p.e. participating in the anode charge formation one can use the

SER function $f_1(x)$ to construct response to any number of primary p.e. $f_N(x)$ using recurrent formula:

$$f_N(x) = f_{N-1}(x) \otimes f_1(x), \tag{20}$$

The parameters in $f_1(x)$ have to be defined with the procedure described in section 3. Taking into account the assumption of Poisson distribution of the registered p.e. number, the fitting function for a measured charge spectrum can be written:

$$f(x) = \sum_{N=1}^{N_{max}} P(N) f_N(x) + P(0) f_p(x), \tag{21}$$

where $P(N)$ is the Poisson distribution probability to have precisely N p.e. in an event with a mean p.e. number μ, and $f_p(x)$ is the noise function.

For $N > 2$ instead of (20) a gaussian approximation of $f_N(x)$ functions can be used, just as in (14), with a resulting χ^2 as good as using (20) (see next section for details).

5 Data analysis

The data analysis of the measurements taken with different filters have been performed using the four methods mentioned above. The results of the analysis are presented in table 5 and discussed in the next subsections.

We aimed to achieve 1% accuracy in our measurements, so we keep significant numbers for all the data in table 5 at this level of accuracy. We estimated the accuracy only for the $P(0)$ method (see appendix B) directly. It is difficult to estimate the precision of the other methods in such a direct way but one can see from table 5 that the different methods give equal results within the claimed accuracy.

5.1 The SER parameters

In order to obtain with a satisfactory precision the SER parameters a high statistics data sample of $1.8 \cdot 10^8$ laser triggers was taken with a $\tau = 0.001$ optical filter. Using the procedure described above we obtained the following numbers.

1. The number of events under the SER histogram after pedestal rejection was $N_{ev} = 3.725 \cdot 10^6$. The mean number of photoelectrons was calculated to be:

$$\mu = -ln\Big(1 - \frac{3.725 \cdot 10^6}{1.8 \cdot 10^8}\Big) = 0.021,$$

since $N_{ev} = N_{triggers}(1 - P(0))$.

2. With μ fixed to 0.021 the fit has been performed with the function (14) (see fig. 3).

3. Using the fit, the pedestal events number have been estimated, leading to the precise evaluation of the number of p.e., which however resulted virtually unchanged (indeed the new evaluation turns out to be 0.0211). It can be seen in the fig. 4 that we have a certain amount of small positive amplitude pulses near x_p. These signals are registered when the trigger hits just after the big amplitude dark event pulse (which has posiive overshoot) has occurred. These pulses should be considered as no-p.e. events.

4. Correction of SER parameters using (15-16) have been performed.

5.2 The attenuator calibration

In order to increase the dynamical range of the ADC an attenuator has been used before the amplifier as shown in fig. 1. Using a precise charge generator (LeCroy mod. 1976) the calibration of the ADC for the attenuator set at 0, 10, 20 and 30dB respectively has been performed. For every set of data a linear fit has been done. The pedestal, measured with high statistics, has been taken as the constant parameter of the fitting linear function. Finally, the calibration of the attenuator has been obtained as the ratio of the corresponding slopes.

5.3 No photoelectrons event number estimation

Together with the pedestal rejection procedure described in the subsection 3.2 (first column in table 4), two alternative methods have been tried.

1. We fixed a value averaging the SER around $x_p + 5\sigma_p$ with a spread of $\pm\sigma_p$, then we rejected the events under the measured charge spectrum for $x > x_p + 5\sigma_p$ plus the events under the rectangular area from x_p up to $x_p + 5\sigma_p$. The mean p.e. number for different measurements are listed in table 4 in the second column.

2. Fitting the pedestal with a Gaussian, we took as pedestal events the normalization factor N_{ped}. The mean p.e. number, obtained with this method of pedestal rejection, for different measurements are listed in table 4 in the third column.

The first method gives better results evaluating the pedestal. Nevertheless the second one, easier to implement, gives results in acceptable agreement in comparison with the former.

5.4 Mean photoelectrons number estimation using SER mean value

Having evaluated x_1 (the mean value of the SER) one can estimate μ from (17). Data are presented in table 5.

We should note that, because of the asymmetrical shape of the SER, x_1 is less than x_0, the main peak position. For a sample of 40 PMTs tested during the preparation of the C.T.F. [10] this difference was in the range of 0-15%. So it is not correct to calibrate the PMTs using x_0.

Here we would like also to point out another difficulty which arises from the non-equivalence of x_0 and x_1. Not knowing apriori the x_1 value which should be defined in the complicated enough way described before we adjust the PMT operating high voltage in order to have the gain factor at $k = 10^7$ at the peak position. It means that the real PMT gain up to 15% less and is equal to $k' = kx_1/x_0$.

5.5 The basis set of the fitting functions

5.5.1 Convolution of the ideal PMT response

A fitting function for the measured charge spectra can be obtained from the known SER_0 function ($f_1(x)$). The SER_0 parameters are obtained by fitting high statistics data. Then the set of discrete functions is constructed as a recursive convolution for every attenuator setting:

$$f_N^0(i) = \sum_{k=1}^{i} f_1^0(k) \cdot f_{N-1}^0(i-k). \tag{22}$$

In fig. 5 and 6 these functions are shown (continuous line) evaluated for 0 and 30 dB respectively. Then the convolution with the gaussian noise function is performed:

$$f_N(i) = \sum_{k=i-10\sigma_p}^{i+10\sigma_p} f_N^0(k) \cdot Noise(i-k). \tag{23}$$

So the final fitting function is:

$$f(i) = N_0\left(\sum_{N=1}^{N_{max}} P(N) f_N(i) + P(0) f_p(i)\right). \tag{24}$$

The data with $\mu \leq 4$ were fitted with four free parameters: the normalization N_0, the mean number of p.e. μ, x_p and σ_p. For $\mu > 4$ when events in pedestal cannot be clearly separated x_p and σ_p were fixed at the measured values. In table 5 we present in the first-last column the values of μ and χ^2 obtained using (24).

Examples of this fitting method are presented in fig. 7 - 10.

5.5.2 Gaussian approximation of basic functions f_N

For big μ (> 4) a gaussian approximation has been tried instead of using the function (24). In this case instead of (23) one should use:

$$f_N(x) = \frac{1}{\sqrt{2\pi}\sigma_N} e^{-\frac{1}{2}\left(\frac{x-x_N}{\sigma_N}\right)^2}, \tag{25}$$

with:

$$x_N = \frac{x_1 N}{k_{att}}, \tag{26}$$

$$\sigma_N^2 = N(\frac{\sigma_1}{k_{att}}) + \sigma_p^2. \tag{27}$$

In fig. 5 and in fig. 6 these gaussians are plotted (dashed lines) for comparison with the functions (23). It can be seen that for a number of p.e. ≥ 3 the gaussian coincide with the corresponding function from (23). One can also see 6 that the noise significantly changes the f_N functions for high k_{att}, so even the SER can be replaced by a gaussian in a noisy enviroment.

Examples of application of this fitting method are presented in fig. 7- 10.

For $0.05 < \mu < 1$ a combined method has been used: as $f_1(x)$ was chose the SER function and for each $f_N(x)$ $(N > 1)$ were chose gaussians as in (25). In table 5 (last column) we present the values of μ and χ^2 obtained using only gaussians or SER plus gaussians (**).

An example of application of this fitting method is presented in fig. 11.

5.6 The quality of the fit

The results of this method are reported in the 7th column of table 7. The quality of the fit was checked by three criteria:

1. χ^2 method;
2. comparison with the μ value obtained by the other methods;
3. the μ value obtained for the different attenuator setting should be the same.

The convolution method is good for $\mu \geq 0.05$ and up to $\mu \simeq 10$ then it gives slightly smaller values due to the accumulated errors while constructing the f_N functions. The gaussian approximation gives good results starting from $\mu > 1$ (even if χ^2 is big), and it is definitely better for high μ values ($\mu > 10$). For $0.05 < \mu < 1$ the combined method gives results comparable with the convolution one.

5.7 Estimation of μ using the relative variance

Estimation of μ using formula (19) for $\mu > 4$ gives significantly different values in comparison with the other methods used (see table 2). The possible reason should be the fluctuations in the electron collection, electrons transfer efficiency etc. In the case of normal distribution (it is also true for Poissonian distribution) of the emitted light one can take into account this fluctuations as [6]:

$$v = v(p) + \frac{1 + v_1}{\mu}, \tag{28}$$

where $v(p)$ is the relative variance of the photoelectrons transfer efficiency.

Fitting the data using (28) with v_1 fixed, we obtained $v(p) = 8.7{\cdot}10^{-3}$, which is a too small value to influence the estimation of small μ, but it becomes noticeable for a bigger μ.

In table 2 recalculated values for the $\mu \geq 1$ are presented. These are the values which are reported in the summary of table 7, in the 5th column.

5.8 Fit correction for the electrons transfer fluctuations

The effect of the electrons transfer fluctuation should also be taken into account for the proper fitting of the PMT charge distribution for big μ. Indeed, fitting the charge distribution with $\mu \simeq 10$ using the gaussian approximation the σ of the fitting curve tends to be slightly less than the experimental value (see fig. 12). Fluctuations in the transfer efficiency will lead finally to increase the distribution spread, in order to account for it we introduce the additional parameter $v(p)$ [1]:

$$\sigma_N^2 = N(\sigma_1^2 + \mu x_1^2 v_p) + \sigma_p^2. \tag{29}$$

We implemented the fit using (29) for charge distributions with $\mu > 4$. In table 3, where the fitting results are presented, one can see that $v(p) \sim 7 \cdot 10^{-3}$. An example of the fit is presented in the fig. 13, the quality of the fit is better, though the μ values remains almost unchanged. This is a consequence of the Poisson character of the primary electrons counting, which is the main assumption in the fitting function. The last column of table 7 reports the results obtained with such correction.

6 Conclusions

The assumption of the Poisson distribution of the detected p.e. number proved to be reasonable for our experimental conditions, as well as the model chose for a SER. In the fig. 15 is presented the logarithmic plot where the estimated p.e. number is shown in dependence on the filters transmittancy. All the methods give the values that are in a good agreement with expected linear dependence of the p.e. number registered on the filter transparency. The figure demonstrates the linearity of the setup in the wide dynamic range of 0.02-20 p.e.

The best way of the mean p.e. number estimation in the $0.2 < \mu < 5$ range in an experimental conditions (when the variations of the light transfer efficiency are bigger then in the laboratory setup) is the fit of the PMT charge distribution with a function (A6) of appendix A with x_0,σ_0,p_E and A values fixed to the values found during the independent PMT calibration and with free μ and v(p). The advantage of the fitting method is its ability to restore μ from "cut" charge distribution (see fig. 9).

The most flexible method of the SER calibration is the use of Poisson probability P(0) in the $\mu \simeq$1-2 p.e.

In the case when the independent calibration was not performed the functions of appendix A can be used with free parameters in order to estimate the x_1 parameter (using Appendix A formula). This will need a bigger statistics.

[1] It is easy to check that the same distribution spread will provide the use of the following formulae:

$$\sigma_N^2 = N(\sigma_1^2 + (N-1)x_1^2 v_p) + \sigma_p^2. \tag{29a}$$

$$\sigma_N^2 = N\sigma_1^2 + \mu^2 x_1^2 v_p + \sigma_p^2. \tag{29b}$$

The (29) has been chosen after the analysis of the fit quality (see 5.6)

If the charge distribution has no cut and the SER (or x_1 parameter) is known the mean p.e. number can be estimated dividing the mean of the distribution by the calibration value x_1(position of the mean for a "pure" SER).

7 Acknowledgments

We would like to thank the I.N.F.N. for supporting this work, Roberto Scardaoni and Francesco Sacchetti from I.N.F.N. Milan, Albert Sotnikov from J.I.N.R. for their contribution in the realization of the experimental set-up.

A Function for the PMT response fitting for the $\mu \simeq 1$

The formula (14) can't be implemented to fit the PMT response to the light source with intensity of $\simeq$ 1 p.e. because of the approximate character of the estimation of the x_1 and σ_1. These quantities can be estimated precisely in our model as:

$$x_1 = (x_0 + \frac{\sigma_0}{\sqrt{2\pi} g_N} exp(-\frac{1}{2}(\frac{x_0}{\sigma_0})^2)(1 - p_E) + p_E \cdot A \qquad (A1)$$

$$\sigma_1^2 = (x_0^2 + \sigma_0^2 + \frac{x_0 \sigma_0}{\sqrt{2\pi} g_N} exp(-\frac{1}{2}(\frac{x_0}{\sigma_0})^2)(1 - p_E) + 2 p_E \cdot A^2 - x_1^2 \qquad (A2)$$

where g_N is normalization factor taking into account the cut of the gaussian part of the SER spectra:

$$g_N = \frac{1}{2}(1 - erf(-\frac{x_0}{\sqrt{2}\sigma_0})) \qquad (A3)$$

Another problem arises from the substitution of the multiple p.e. responses with gaussians. While for $n \geq 3$ the gaussian is a very good approximation (see fig.5), there is a significant deviation from the gaussian shape in the n=2 response. Precise analytical formula for the $f_1 x f_1$ convolution is quit complicated and its use in the fitting procedure slows down the calculation. The following approximation can be obtained neglecting the smallest contributions (x should be replaced by $x - x_p$ in the right part of the equation in the case of non-zero pedestal value):

$$f_2(x) = {p_E}^2 \frac{x}{A^2} e^{-\frac{x}{A}} + 2\frac{(1 - p_E) p_E}{\sqrt{2\pi}\sigma_0} exp(-\frac{1}{2}(\frac{x - x_0 - A}{\sigma_0})^2) + \frac{(1 - p_E)^2}{2\sqrt{\pi}\sigma_0} exp(-\frac{1}{2}(\frac{x - 2x_0}{\sigma_0 \sqrt{2}})^2) \qquad (A4)$$

This approximation provide $\simeq$ 1% precision in the parameters region typical for our PMT ($0.1 < p_E < 0.2$, $\frac{x_0}{10} < A < \frac{x_0}{5}$, $\sigma_0 \simeq \frac{1}{\sqrt{2}} x_0$).

The last problem of the correct PMT charge spectra fitting is taking into account the photons transfer efficiency v(p) (including all the possible variations of the photocathode quantum efficiency from point to point and from the angle of incidence etc.) One can neglect this variations only for

$$\mu << \frac{1 + v_1}{v(p)} \qquad (A5)$$

For a big enough μ when parameter v(p) is not known it is better to leave it free and use formula (29) for σ_N.

The fitting function for a measured charge spectrum can be written as:

$$f(x) = P(0)f_p(x) + P(1)f_1(x) + P(2)f_2(x) + \sum_{N=3}^{N_{max}} P(N)f_N(x), \qquad (A6)$$

where $P(N)$ is the Poisson distribution and $f_p(x)$ is the noise function. For the functions $f_N(x)$ the gaussian approximation (with parameters defined by (A1) and (A2) is used. $f_1(x)$ function coincide with SER(x) function (8).

The function has been tested on the CTF data (runs with a Rn source at the center). On the statistics of $\simeq 80,000$ events it gives fit with $\chi^2 \simeq 0.9 - 1.1$. Parameter v(p)$\simeq 0.025$ in CTF is significantly bigger than at the lab conditions reflecting the fact of the more complicated nature of the light transfer in CTF.

In order to check stability of the fit the 64 samples of 40,000 events each have been acquired in the lab for the same PMT in the same conditions with $\mu = 2.15$ (defined from the combined statistics with a high precision following the procedure described in 3.2). The fit of the each sample has been performed. Parameters of the fit variates around their mean values as (with 1σ errors):

$$< \mu >= 2.151 \pm 0.026;$$

$$< v_1 >= 0.294 \pm 0.014;$$

$$< x_1 >= 244 \pm 2.$$

So we can conclude that 40000 statistics with $\mu \simeq 2$ is enough to obtain SER calibration parameters with a 1% precision at the 1σ c.l.

If the parameters of SER (x_0,σ_0,p_E and A) are fixed to the values obtained in independent high statistics calibration and only the parameters μ,$v(p)$,x_p and σ_p are free, the fit of the same data samples gives

$$< \mu >= 2.147 \pm 0.009,$$

providing even better estimation of the μ value.

B Appendix: The accuracy of the mean p.e. number calculation from the amount of no-p.e. events

The estimation of the mean number of p.e. from the amount of the events in the pedestal is based only on the assumption of the Poisson-like distribution of the p.e. registration statistics. This means we do not take into account the linearity of the PMT, which is an important point when all the other methods described in this paper but this one are concerned.

However, while implementing this technique, errors can arise in separating small amplitude pulses from pedestal events (no-p.e. events). Here we suppose that pedestal events are separated perfectly.

The mean p.e. number is estimated from:

$$\mu = -ln\Big(\frac{N_{ped}}{N_{trigger}}\Big). \qquad (B1)$$

Let us call P_0 the probability to have a no-p.e. response, then $1 - P0$ is the probability to have a p.e. response. Because of the Poisson law of the registrated p.e.:

$$P_0 = e^{-\mu}. \qquad (B2)$$

Therefore we have a simple binomial law for the probability of having a signal under the pedestal. The mean value and the r.m.s. for this binomial distribution are, respectively:

$$< N_{ped} >= N_{trigger} \cdot P_0, \qquad (B3)$$

and

$$\sigma^2_{N_{ped}} = N_{trigger} \cdot P_0 \cdot (1 - P_0). \qquad (B4)$$

For a 1σ error estimation we can substitute N_{ped} with $N_{ped} \pm \sqrt{N_{triggers}} e^{-\mu/2}\sqrt{1 - e^{-\mu}}$. The error on μ is not symmetrical and it turns out that the bigger error comes out from the substitution of $N_{events} - \sqrt{N_{events}} e^{-\mu/2}\sqrt{1 - e^{-\mu}}$. Performing this substitution and taking we have:

$$\mu + \Delta\mu = -ln\Big(e^{-\mu} - \frac{1}{\sqrt{N_{trigger}}} e^{-\mu/2}\sqrt{1 - e^{-\mu}}\Big). \qquad (B2)$$

For 1% accuracy at 1σ c.l. $\Delta\mu$=0.01μ and as a consequence

$$N_{trigger} = \frac{1 - e^{-\mu}}{e^{-\mu}(1 - e^{-0.01\cdot\mu})^2}. \qquad (B3)$$

In fig. 14 the number of triggers for a 1% accuracy at 1σ and 3σ c.l. is shown.

C Appendix: Corrections to the SER parameters to account for multip.e. hits ($\mu \ll 1$)

After the pedestal rejection the contribution of multiple p.e. remains in the charge spectrum. One can easily obtain the corrected values for x_1 and $signa_1$ supposing the Poisson distribution of the detected p.e. number and the PMT linearity.

The mean value of the ADC spectrum with the multiple p.e. contribution is:

$$x^*_m = x_1 \cdot \frac{\mu}{1 - P(0)}, \qquad (C1)$$

where x_1 is the mean value of the SER and the normalization does not contain P(0) because of the pedestal rejection. Taking into account the condition $\mu \ll 1$, the correction on x_1 can be obtained from (C1):

$$x_1 = x_m^*(1 - \frac{\mu}{2}). \qquad (C2)$$

In order to define the relative variance:

$$v^* \equiv \left(\frac{\sigma_m^*}{x_m^*}\right)^2 = \frac{< x^2 >}{< x >^2} - 1. \qquad (C3)$$

one should evaluate $< x^2 >$ (averaging over the spectrum without pedestal):

$$< x^2 >=< x >^2 + (\sigma_m^*)^2 =$$

$$= \frac{P(1) \cdot (x_1^2 + \sigma_1^2) + P(2) \cdot (4x_1^2 + 2\sigma_1^2) + \dots}{P(1) + P(2) + \dots} =$$

$$=< n > \cdot \frac{\sigma_1 + (1 + < n >)x_1^2}{1 - P(0)}. \qquad (C4)$$

where $< n >\equiv \mu$ and $< n >=< n^2 > - < n >^2$ (Poisson ditribution).

Therefore the relation between v^* and v_1 is:

$$v^* = (v_1 + 1) \cdot \frac{1 - e^{-\mu}}{\mu} - e^{-\mu}. \qquad (C5)$$

Taking into account the condition $\mu \ll 1$ the corrected value of v_1 can be obtained from (C5):

$$v_1 = v^* \left(1 + \frac{\mu}{2}\right) - \frac{\mu}{2}. \qquad (C6)$$

References

[1] J. Veloso and C.A.N. Conde, IEEE Transaction on Nuclear Science, Vol. 40 (1993).

[2] A.G. Wright, IEEE Transaction on Nuclear Science, Vol.34, No.1, February 1987.

[3] A.G. Wright THORN EMI Electron Tubes Limited, Photodetection Information Service *Source of noise in photomultipliers.*

[4] B.H. Candy Rev. Sci. Instrum. 56(2), 1985.

[5] P.B. Coates J. Phys. D: App. Phys., Vol. 6, 1973.

[6] J.B. Birks, The Theory and Practice of Scintillation Counting, Pergamon Press.

[7] E.H. Bellamy et al. NIM A339(1994) 468-476

[8] V. Cavasinni et al. ATLAS Internal Note TILECAL-NO-117

[9] Philips PMTs book

[10] Borexino Collaboration, Ultra-low measurements in a large volume underground detector, in publication on Astroparticle Physics.

TABLES

Filters properties		
Density D	**Transmission τ**	**τ tolerance**
0.3	0.5	5%
0.7	0.2	5%
1	0.1	5%
1.3	0.05	10%
1.7	0.02	10%
2	0.01	10%
3	0.001	20%

Table 1: *Declared optical filters properties*

$\mu = x_m/x_1$	$\mu = (v_1 + 1)/v$	$\mu = (1 + v_1)/(v - v(p))$
1.10	1.08	1.09
1.32	1.30	1.32
2.05	2.07	2.10
2.09	2.10	2.14
4.21	3.91	4.02
10.3	9.46	10.2
10.4	9.49	10.2
9.85	9.07	9.74
9.95	9.04	9.70
21.7	18.8	21.9
21.8	19.1	22.2

Table 2: *Recalculated values for the relative variance method.*

N_0	μ_I	μ_F	χ^2	$v(p)(10^{-3})$
1	21.8	21.8	1.69	4.7
2	21.8	22.0	1.00	5.4
3	10.2	10.3	3.02	7.0
4	10.2	10.2	2.19	7.6
5	10.3	10.4	2.22	7.5
6	9.8	9.85	2.25	6.2
7	9.7	9.76	2.13	8.2
8	9.9	9.00	2.26	8.6
9	4.07	4.23	2.25	7.0
10	4.12	4.20	1.70	7.0

Table 3: *Fit with correction for the light transfer fluctuations.* μ_I *for gaussian approximation method* μ_F *for gaussian approximation with* $v(p)$ *as free parameter*

Mean p.e. number for different method of pedestal rejection			
No	**I method**	**II method**	**III method**
1	0.0114	0.0116	0.0101
2	0.0211	0.0212	0.0202
3	0.0224	0.0221	0.0204
4	0.0238	0.0238	0.0230
5	0.0248	0.0249	0.0235
6	0.0548	0.0550	0.0534
7	0.0561	0.0562	0.0541
8	0.0970	0.0973	0.0946
9	0.116	0.116	0.113
10	0.192	0.193	0.189
11	0.188	0.189	0.183
12	0.204	0.201	0.194
13	0.208	0.207	0.205
14	0.409	0.399	0.388
15	0.426	0.428	0.411
16	0.431	0.433	0.425
17	0.436	0.423	0.410
18	1.11	1.10	1.08
19	1.29	1.32	1.30
20	2.06	2.05	1.98
21	2.16	2.09	2.02

Table 4: *Mean p.e. number evaluated by three different methods of pedestal rejection. I method: using the single photoelectron response fitting function to discard real photoelectrons small amplitude pulses. II method: using a suitable cut (see text) to discard real pulses from the pedestal region. III method: fitting the pedestal events with a gaussian.*

Figures captions

FIG.1 Sketch of the experimental set-up

FIG.2 Dark noise and PMT response to a low intensity light source. The dynodes noise spectrum is also shown

FIG.3 The SER charge spectrum taken with a mean p.e. number equal to 0.021. In the upper plot the exponential part and the gaussian one in the SER are shown. The exponential function is convoluted with the noise. The contribution of 2 and 3 p.e. to the PMT response can be seen in the logarithmic scale.

FIG. 4 The pedestal rejection procedure using the single photoelectron fitting function. The SER model function convoluted with the noise circumscribe the black-painted area.

FIG. 5 Set of convoluted and gaussian (dashed lines) functions to work out the phototube charge spectrum fitting for a 0dB attenuator setting.

FIG. 6 As in fig. 5 but for a 30dB attenuator setting.

FIG. 7 PMT charge spectrum fit usign the convolution method (upper plot) and the gaussian one.

FIG. 8 PMT charge spectrum fit using the convolution method (upper plot) and the gaussian one.

FIG. 9 PMT charge spectrum fit using the convolution method (upper plot) and the gaussian one.

FIG. 10 PMT charge spectrum fit using the convolution method (upper plot) and the gaussian one.

FIG. 11 PMT charge spectrum fit using the convolution method (upper plot) and the gaussian one.

FIG. 12 PMT charge spectrum fit using the gaussian approximation. The mean number of p.e. is calculated to be 21.71 and χ^2=2.76.

FIG. 13 PMT charge spectrum fit with correction for the light transfer fluctuations. The mean p.e. number is 21.68 and χ^2=1.80.

FIG. 14 Statistics for 1% accuracy at 1σ and 3σ c.l. for different mean number of p.e.

FIG. 15 Calculated mean p.e. number (x_m/x_1) vs declared transmission as in table 1.

Experimental setup sketch

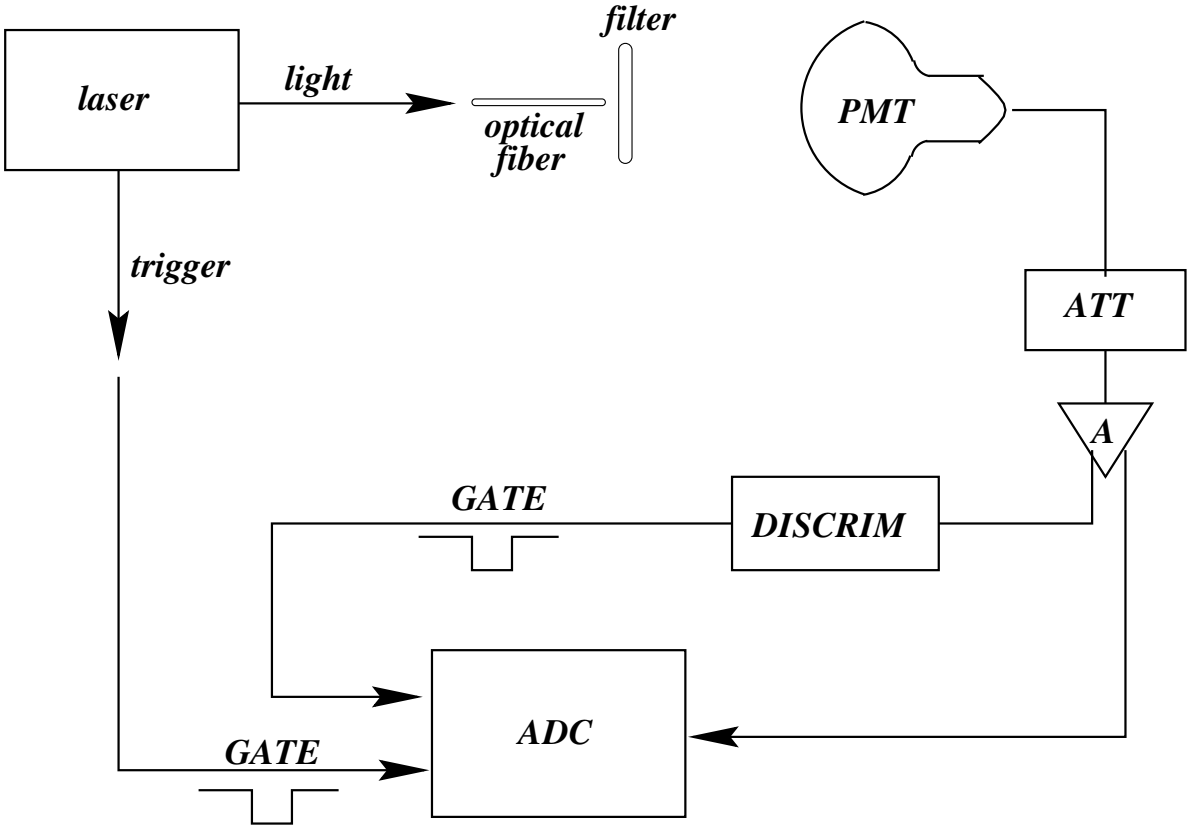

Figure 1: *Sketch of the experimnetal set-up*

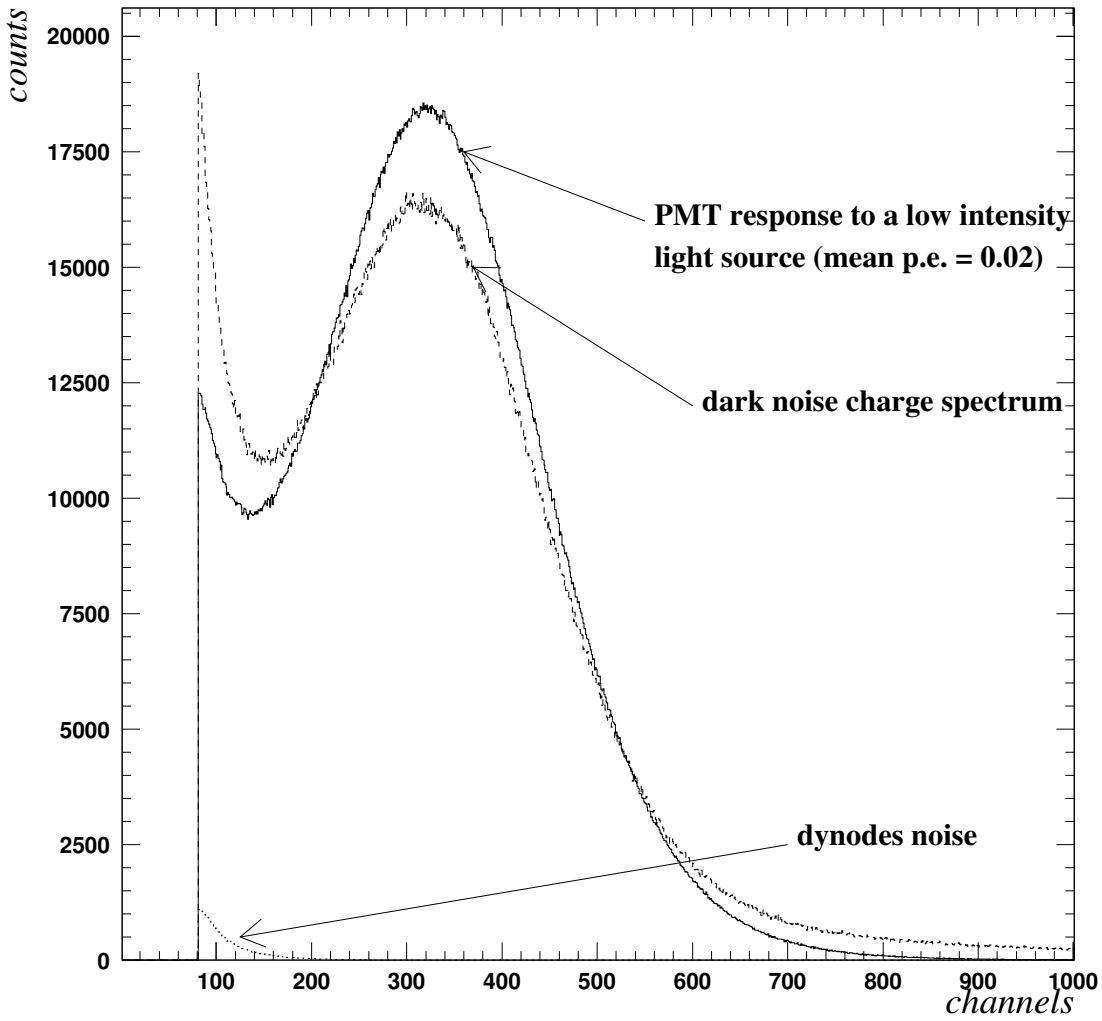

Figure 2: *Dark noise and PMT response to a low intensity light source. The dynodes noise spectrum is also shown*

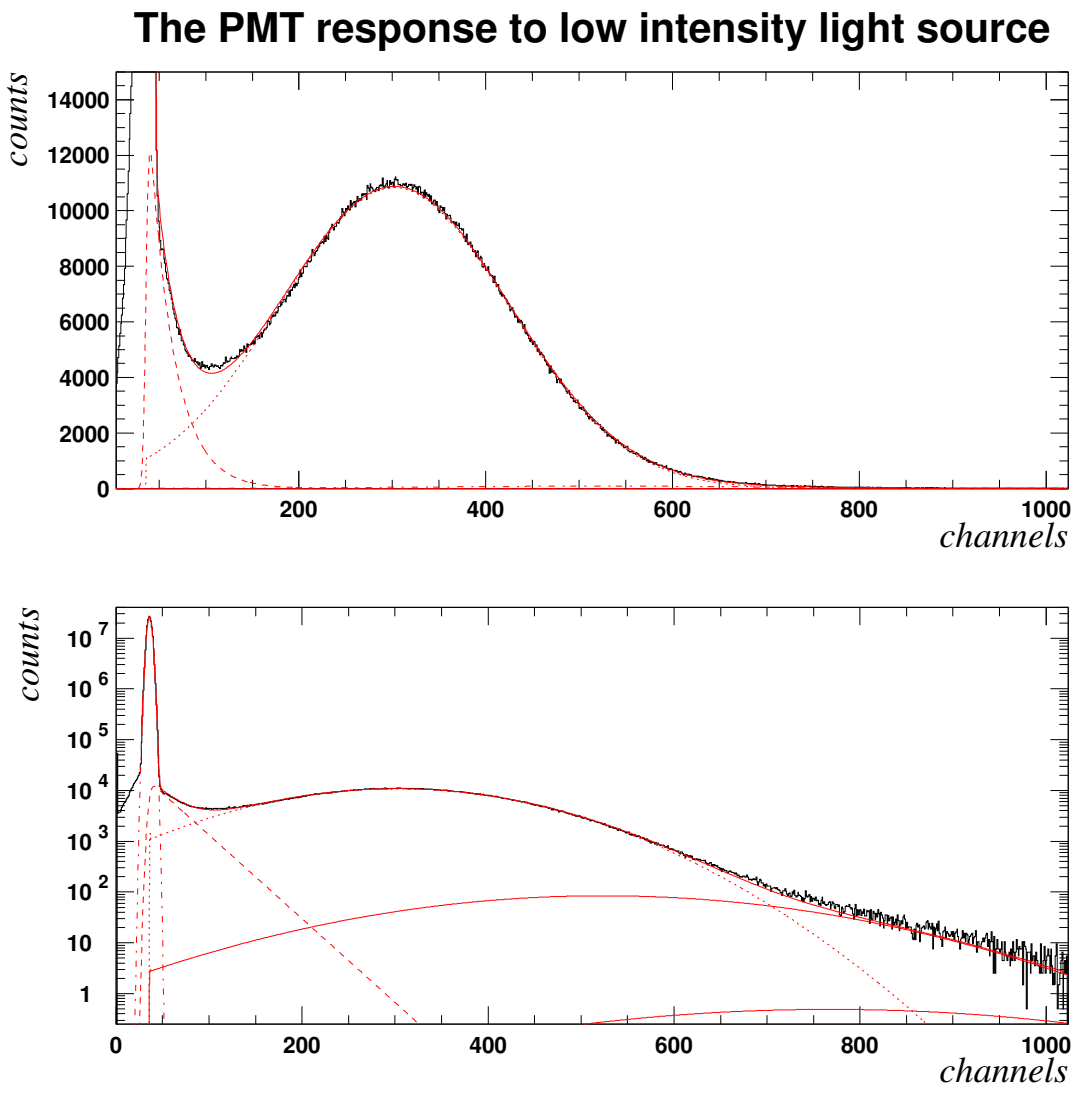

Figure 3: *The SER charge spectrum taken with a mean p.e. number equal to 0.021. In the upper plot the exponential part and the gaussian one in the SER are shown. The exponential function is convoluted with the noise. The contribution of 2 and 3 p.e. to the PMT response can be seen in the logarithmic scale.*

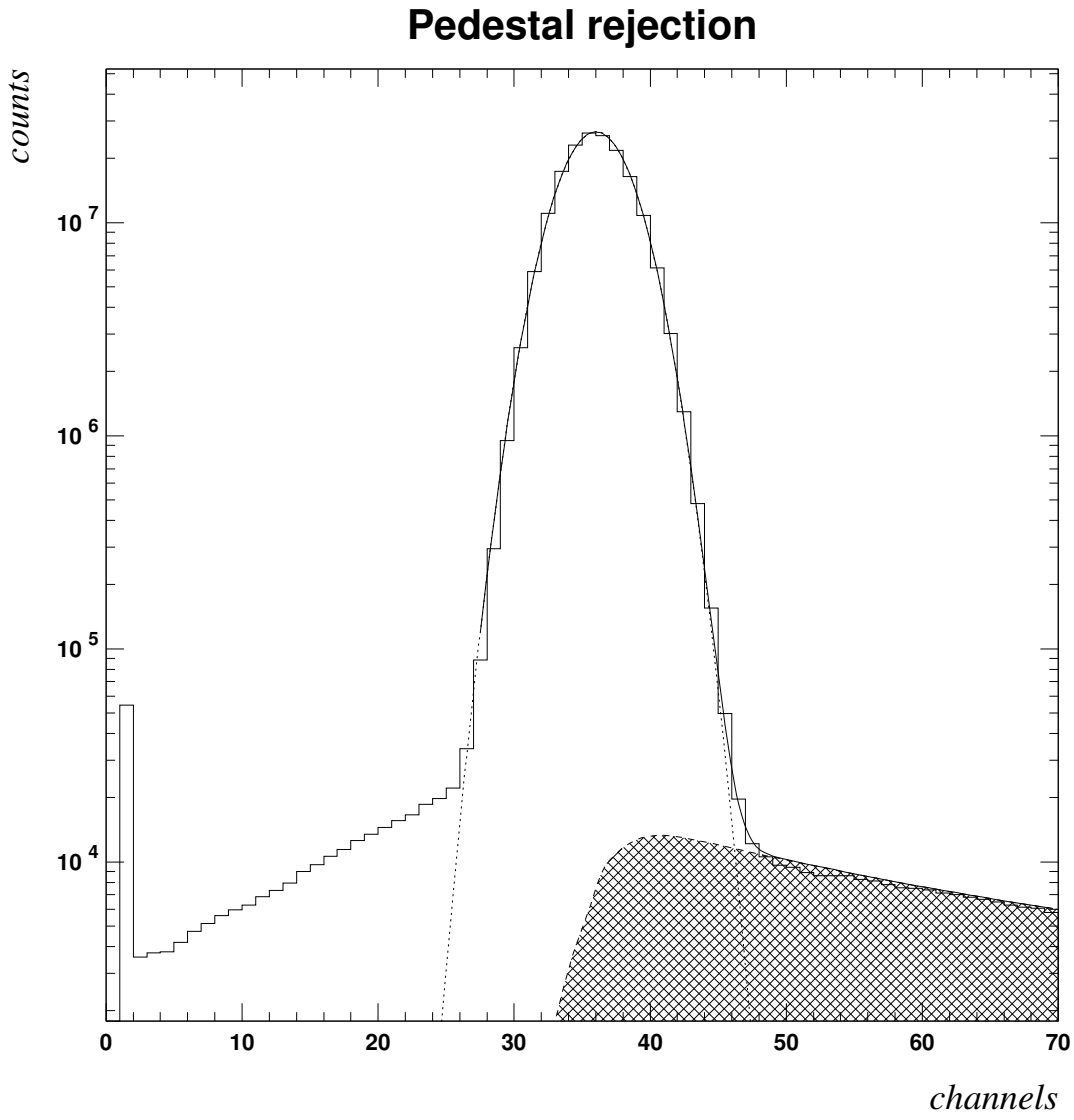

Figure 4: *The pedestal rejection procedure using the single photoelectron fitting function. The SER model function convoluted with the noise circumscribe the black-painted area.*

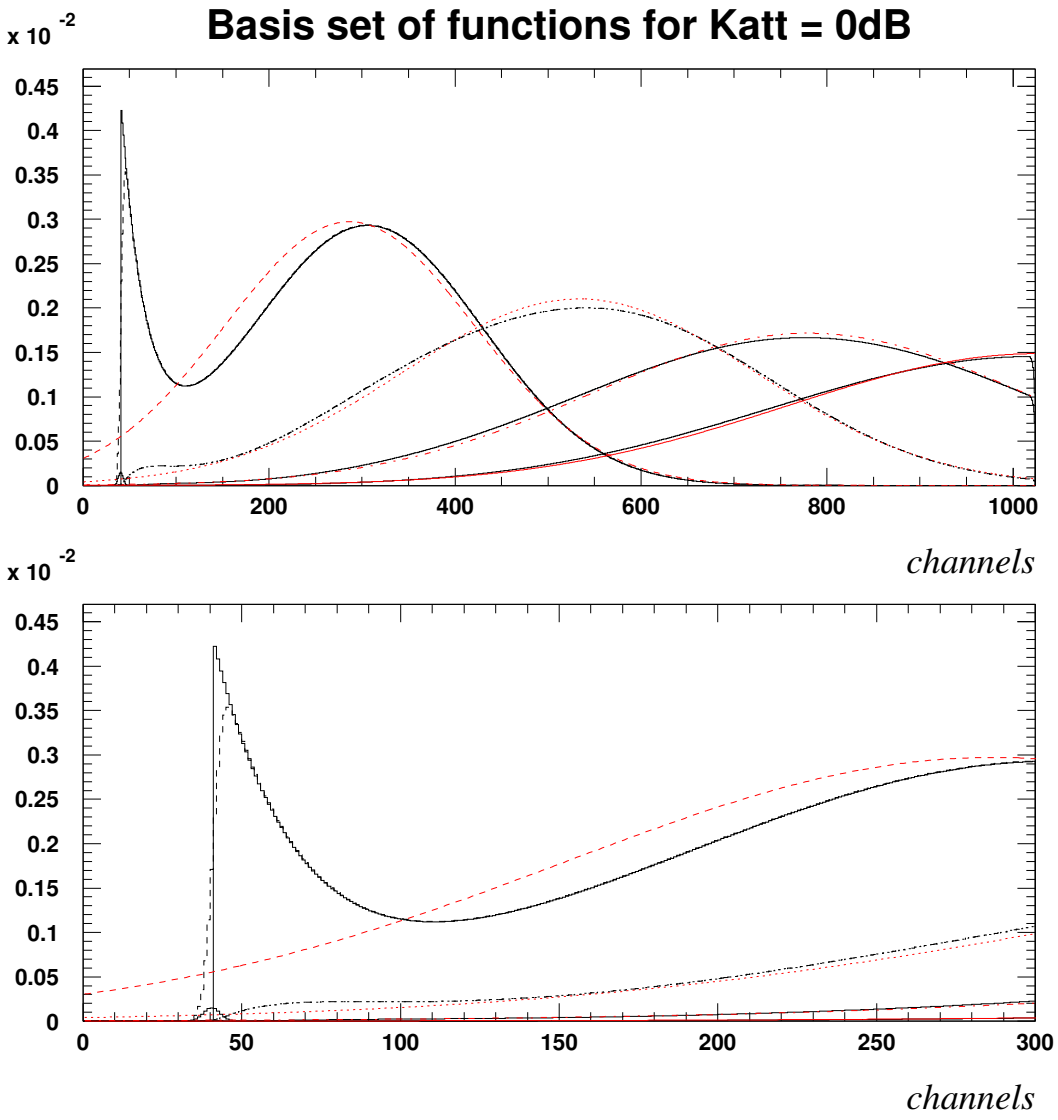

Figure 5: *Set of convoluted and gaussian (dashed lines) functions to work out the phototube charge spectrum fitting for a 0dB attenuator setting.*

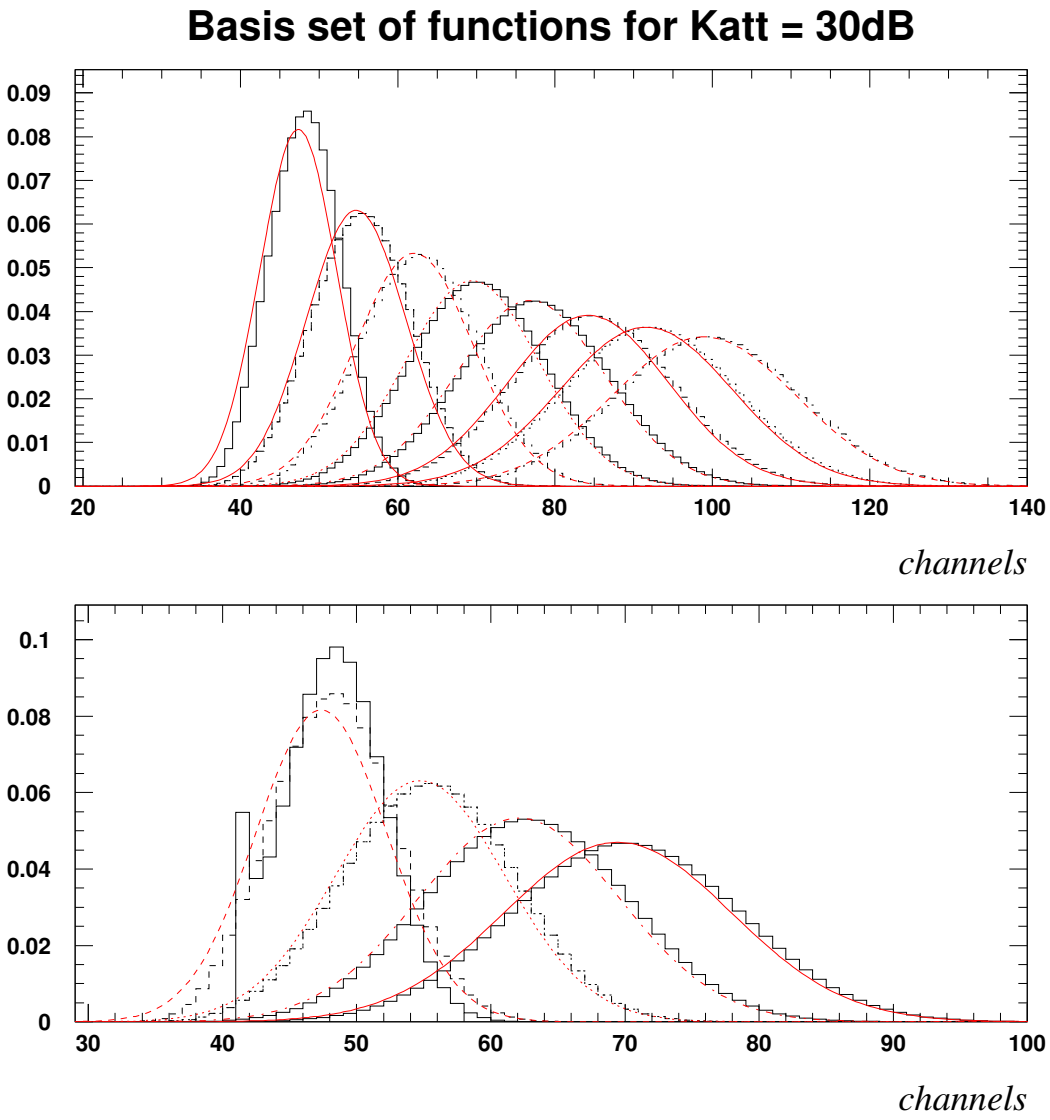

Figure 6: *As in fig. 5 but for a 30dB attenuator setting.*

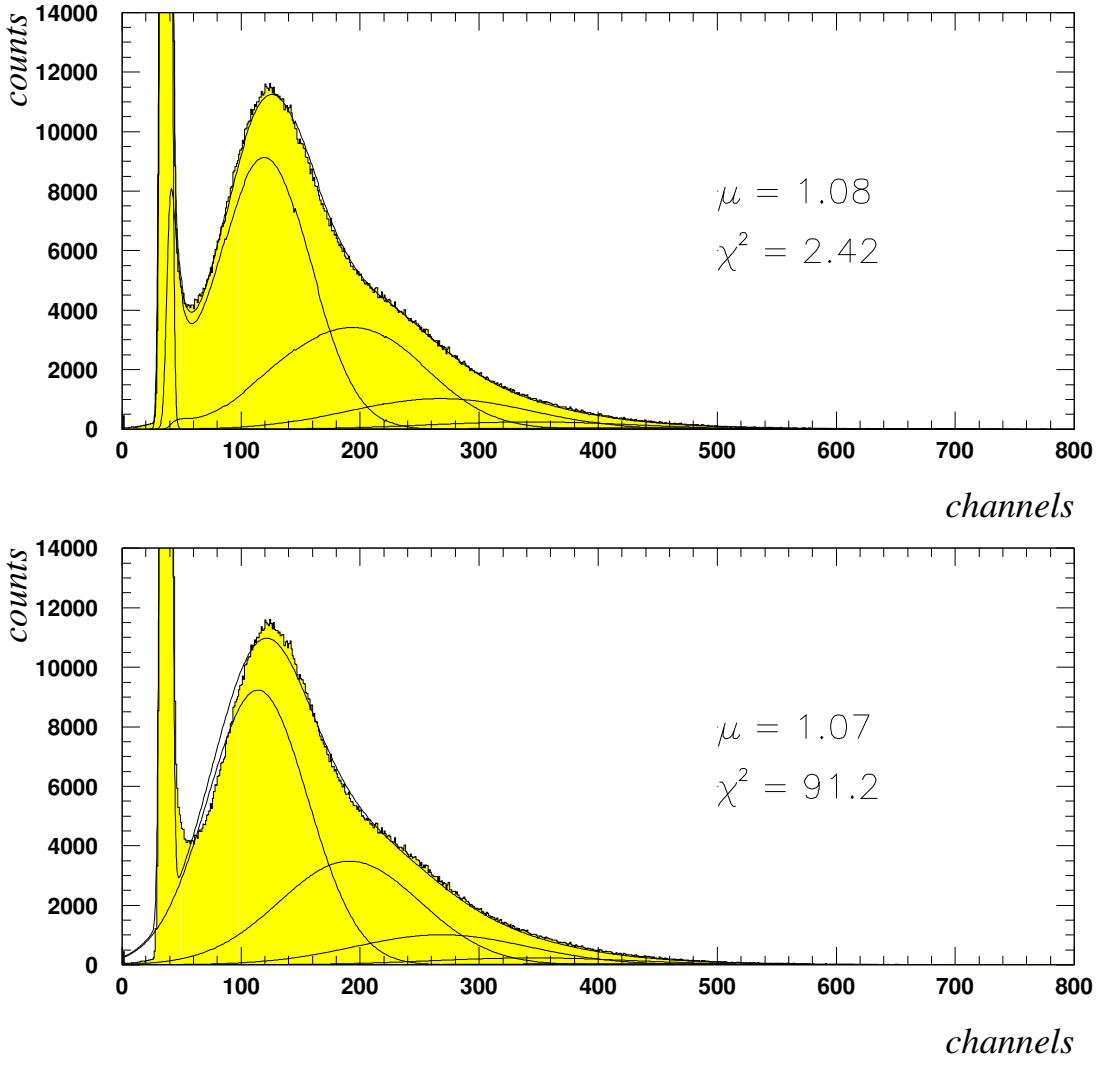

Figure 7: *PMT charge spectrum fit usign the convolution method (upper plot) and the gaussian one.*

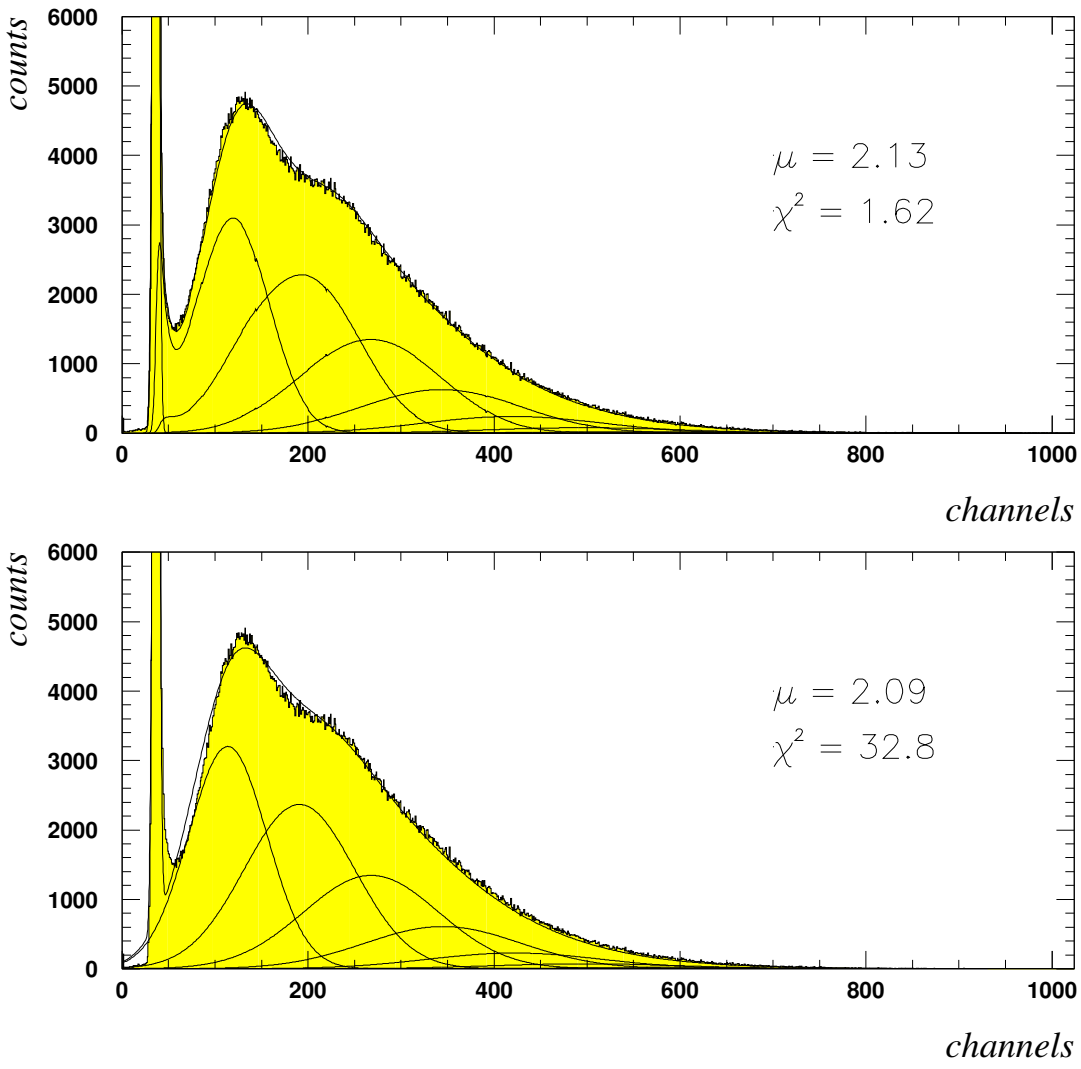

Figure 8: *PMT charge spectrum fit using the convolution method (upper plot) and the gaussian one.*

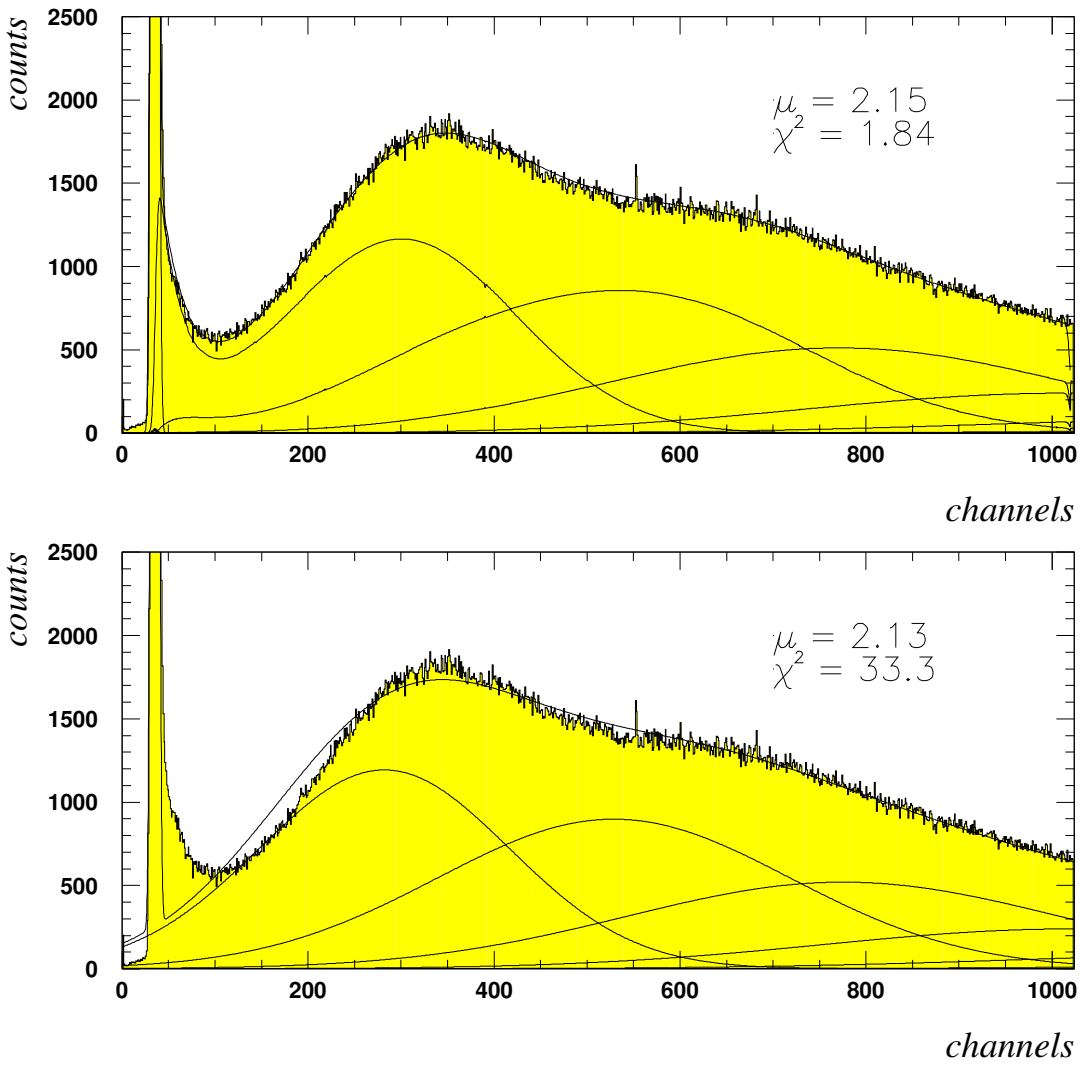

Figure 9: *PMT charge spectrum fit usign the convolution method (upper plot) and the gaussian one*

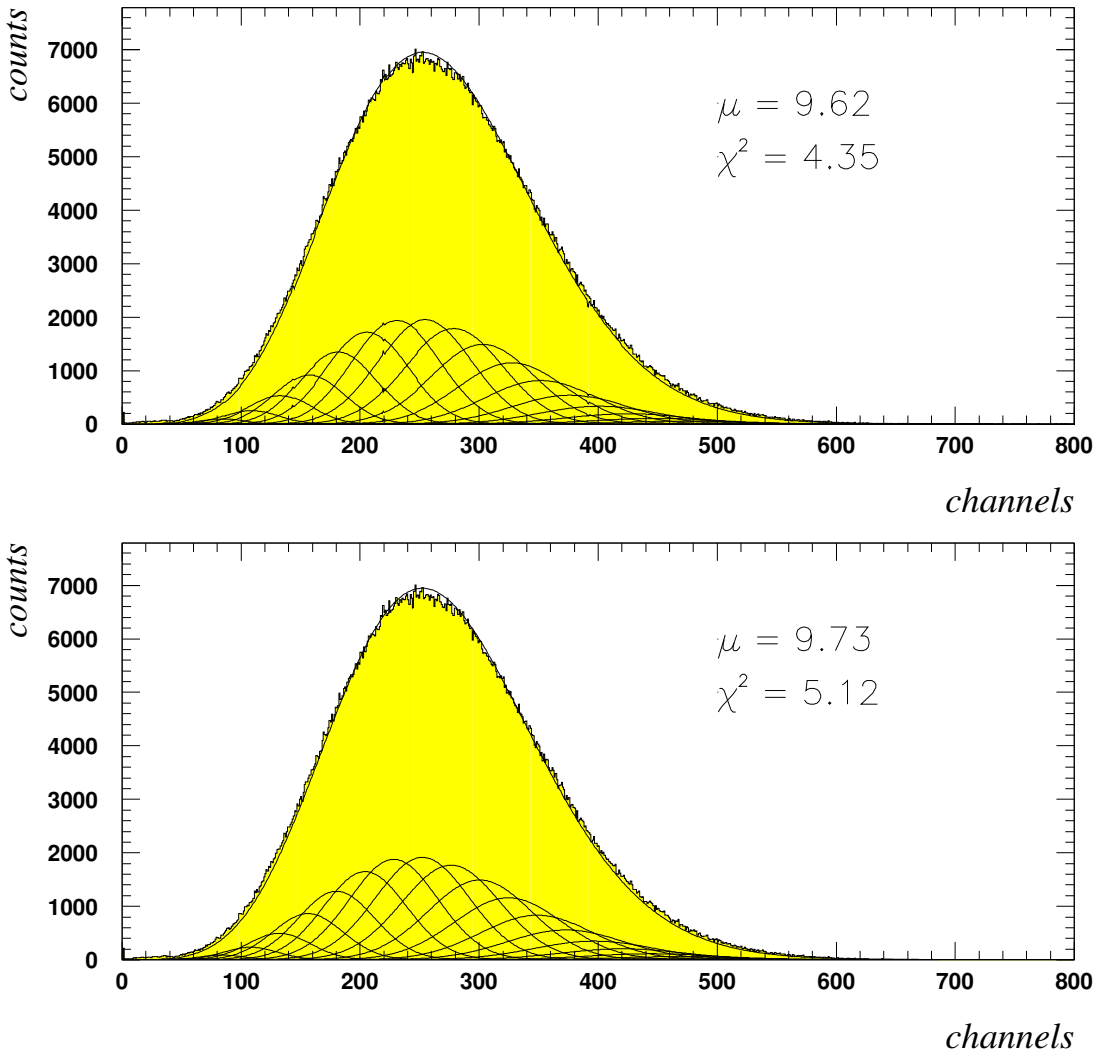

Figure 10: *PMT charge spectrum fit using the convolution method (upper plot) and the gaussian one*

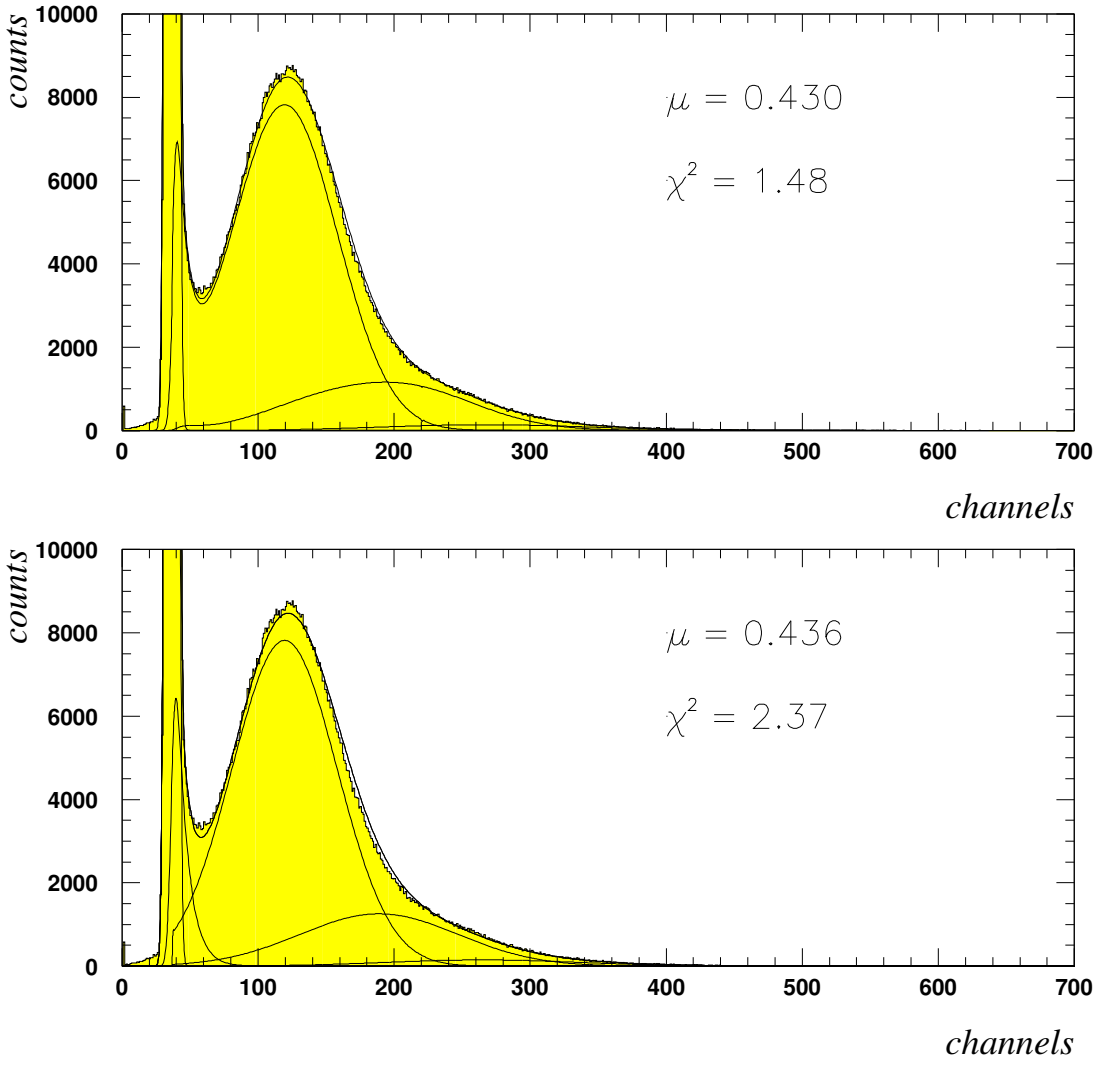

Figure 11: *PMT charge spectrum fit using the convolution method (upper plot) and the combined gaussian one*

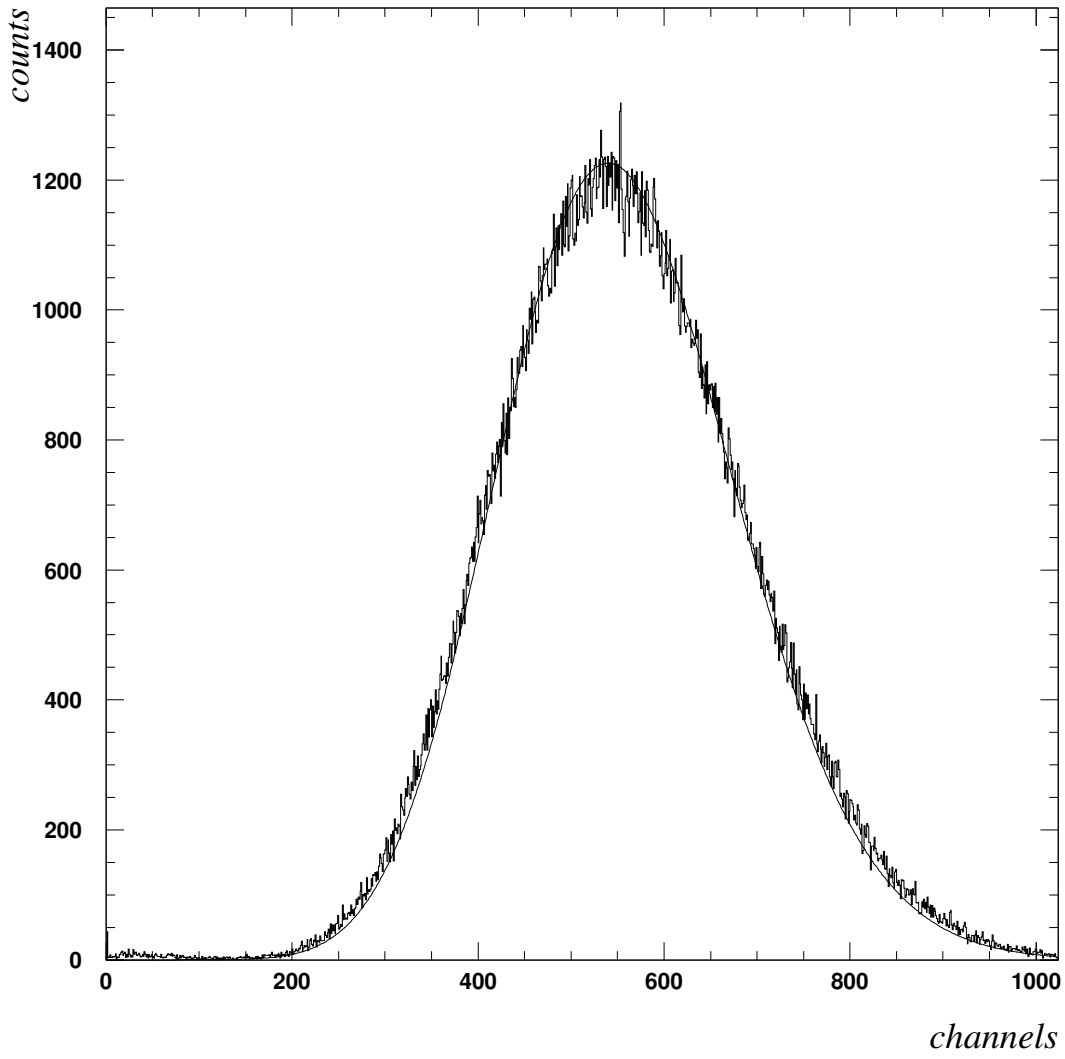

Figure 12: *PMT charge spectrum fit using the gaussian approximation. The mean number of p.e. is calculated to be 21.71 and* χ^2*=2.76.*

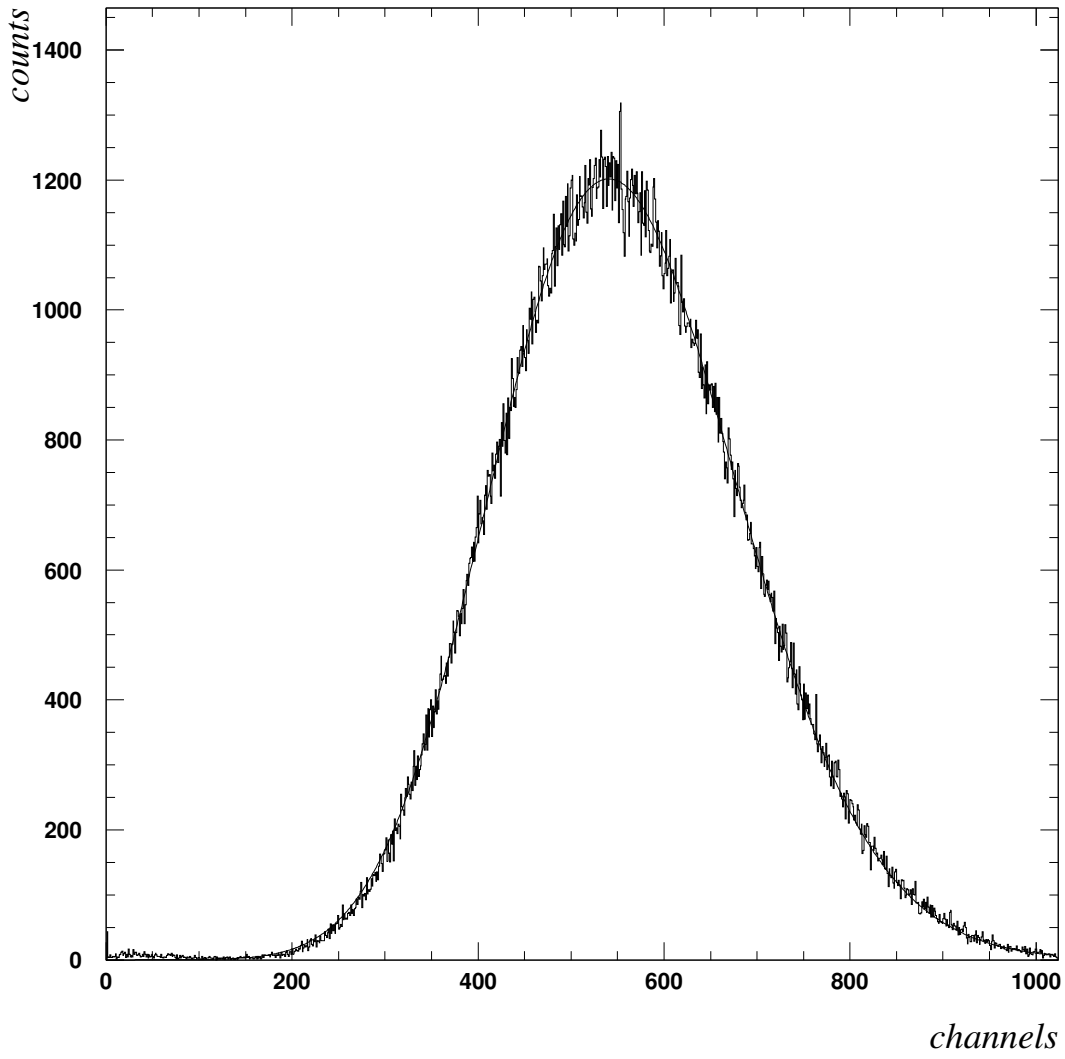

Figure 13: *PMT charge spectrum fit with correction for the light transfer fluctuations. The mean p.e. number is 21.68 and* χ^2*=1.80.*

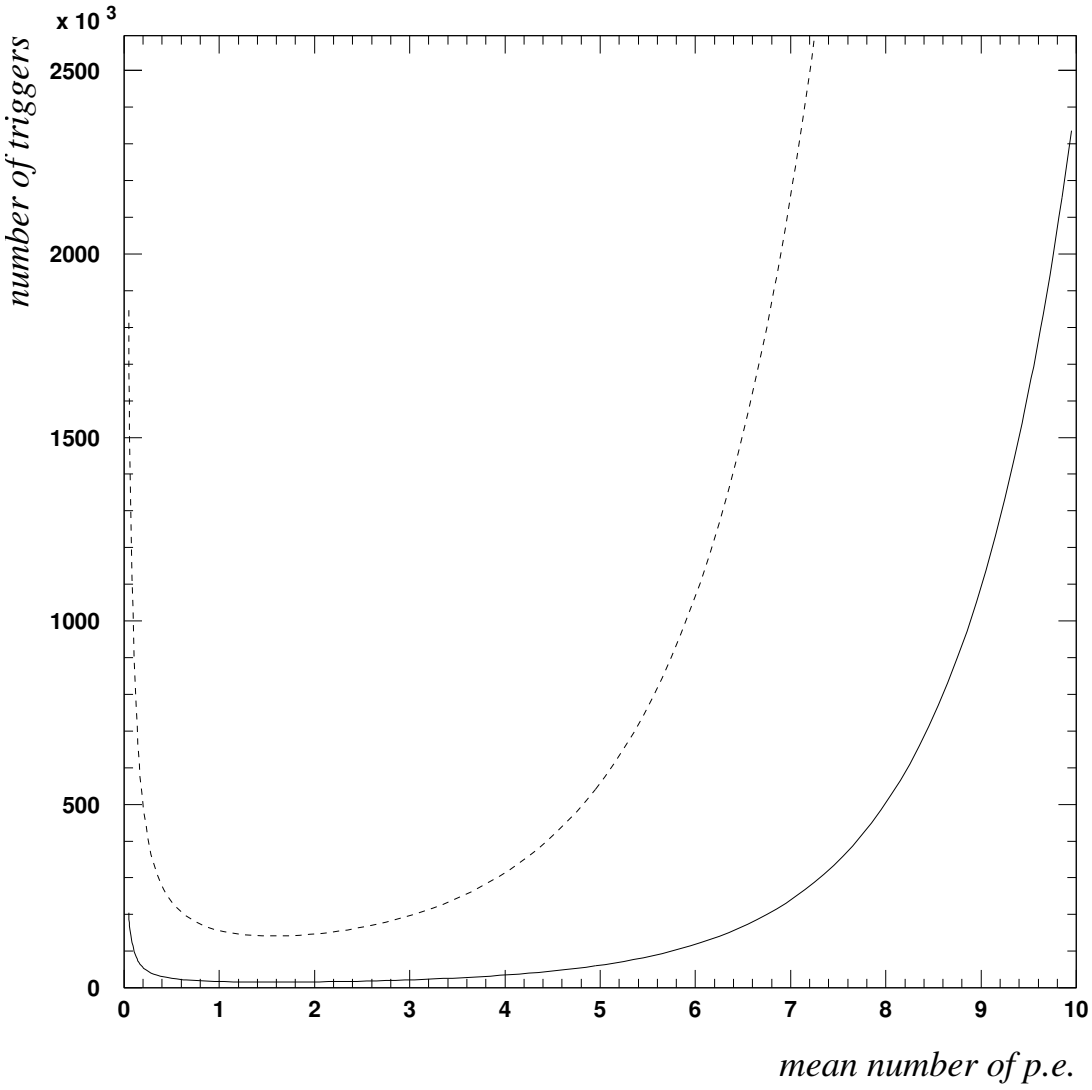

Figure 14: *Statistics for 1% accuracy at 1σ and 3σ c.l. for different mean number of p.e.*

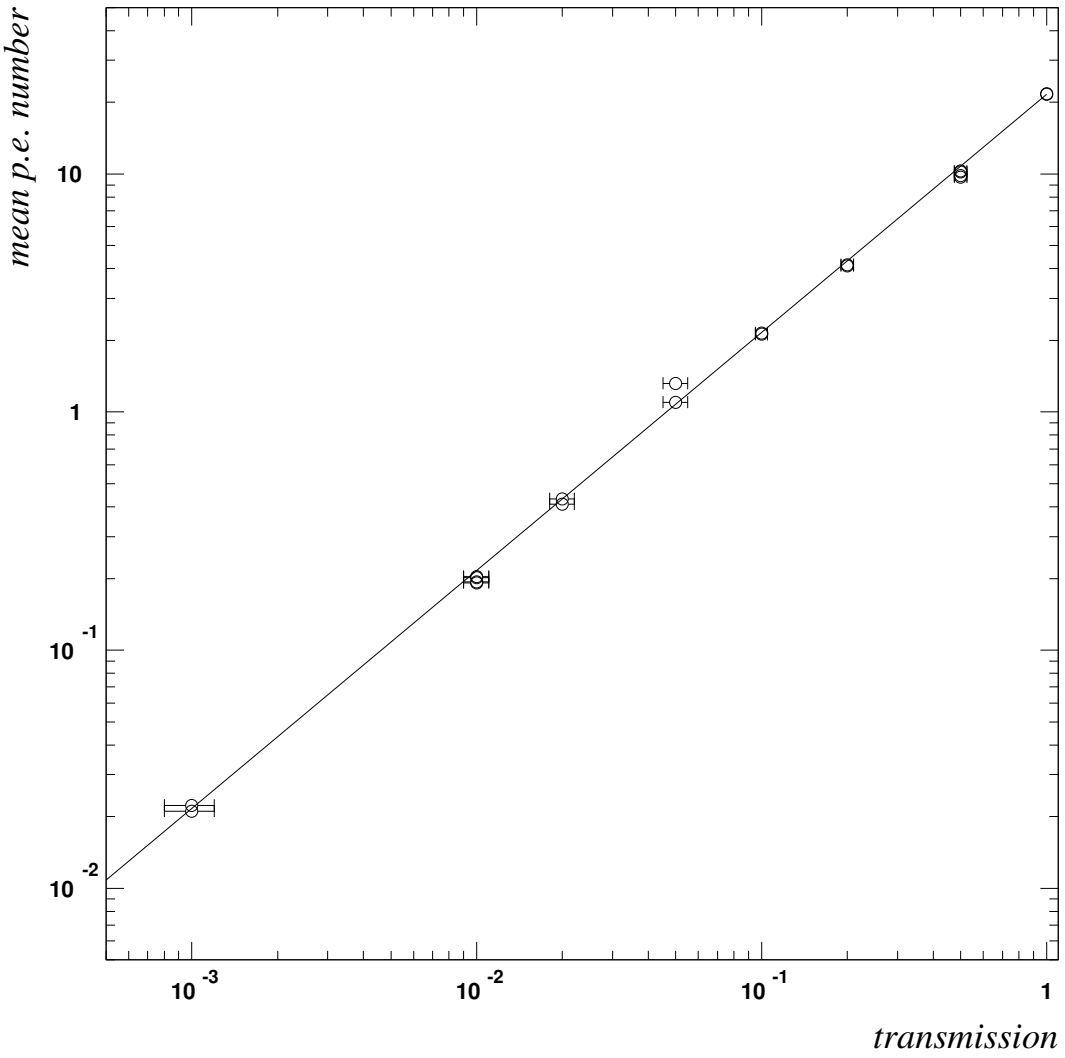

Figure 15: *Calculated mean p.e. number (x_m/x_1) vs declared transmission as in table 1*

No	Att(dB)	$\mu = x_m/x_1$	$\mu = -ln(P(0))$	$\mu = (v_1+1)/(v-v(p))$	fitI(χ^2)	fitII(χ^2)
1	0	0.0113	0.0114	0.0110	L	L
2	0	0.0211	0.0211	0.0211	L	L
3	0	0.0223	0.0224	0.0223	L	L
4	0	0.0223	0.0238	0.0237	L	L
5	0	0.0247	0.0248	0.0247	L	L
6	0	0.0551	0.0548	0.0552	0.0555	L
7	0	0.0564	0.0561	0.0565	0.0567	L
8	0	0.0973	0.0970	0.0975	0.102	L
9	0	0.117	0.116	0.117	0.115(8.19)	0.107(8.09)**
10	0	0.194	0.192	0.195	0.192(8.24)	0.195(8.18)**
11	10	0.192	0.188	0.191	0.192(8.39)	0.197(12.24)**
12	0	0.204	0.204	0.208	0.205(4.42)	0.208(5.05)**
13	10	0.202	0.208	0.204	0.206(2.72)	0.211(5.34)**
14	0	*	0.428	*	0.423(8.29)	0.430(9.10)**
15	10	0.411	0.409	0.408	0.410(1.73)	0.415(3.41)**
16	10	0.432	0.436	0.431	0.430(1.48)	0.436(2.37)**
17	0	*	0.433	*	0.432(7.03)	0.439(7.48)**
18	0	*	1.10	*	1.09(2.28)	1.08(45.2)
19	10	1.10	1.07	1.08	1.08(2.42)	1.07(91.2)
20	0	*	1.32	*	1.32(1.70)	1.31(31.2)
21	10	1.32	1.29	1.32	1.32(1.03)	1.29(40.4)
22	0	*	2.11	*	2.10(1.72)	2.07(36.9)
23	10	2.12	2.06	2.10	2.10(1.69)	2.05(57.6)
24	0	*	2.16	*	2.15(1.84)	2.13(33.3)
25	10	2.15	2.16	2.16	2.13(1.62)	2.09(32.8)
26	0	*	4.03	*	4.07(1.66)	4.02(14.1)
27	10	4.16	L	4.20	4.12(1.25)	4.11(6.84)
28	20	4.12	L	4.11	4.11(2.00)	4.08(4.08)
29	10	*	L	*	9.55(2.99)	9.79(2.58)
30	20	9.70	L	9.68	9.62(4.35)	9.73(5.12)
31	30	9.85	L	9.72	9.81(3.57)	9.89(5.08)
32	10	*	L	*	9.94(4.02)	10.19(4.19)
33	20	10.2	L	10.2	10.13(2.14)	10.20(4.80)
34	30	10.3	L	10.2	10.24(3.48)	10.33(4.78)
35	20	21.7	L	21.7	21.3(1.65)	21.7(2.76)
36	30	21.6	L	22.3	21.6(1.89)	21.9(2.78)

Table 5: *Mean photoelectrons number obtained implementing differents methods. L - too low statistics for the method used; * - histogram cut, i.e. mean value and r.m.s. cannot be defined; ** - while fitting with gaussians the SER is used (combined method - see text)*